WATER RESOURCES RESEARCH, VOL. 31, NO. 4, PAGES 1137–1145, APRIL 1995

Three-dimensional analytical models of contaminant transport from nonaqueous phase liquid pool dissolution in saturated subsurface formations

Constantinos V. Chrysikopoulos

Department of Civil and Environmental Engineering, University of California, Irvine

Abstract. Closed form analytical solutions are derived for three-dimensional transient contaminant transport resulting from dissolution of single-component nonaqueous phase liquid pools in saturated porous media. The solutions are suitable for homogeneous porous media with unidirectional interstitial velocity. The dissolved solute may undergo first-order decay or may sorb under local equilibrium conditions. The solutions are obtained for rectangular and elliptic as well as circular source geometries, assuming that the dissolution process is mass transfer limited, by applying Laplace and Fourier transforms. Although the solutions contain integral expressions, these integrals are easily evaluated numerically. These solutions are useful for verifying the accuracy of numerical solutions to more comprehensive models and for design and interpretation of experiments in laboratory-packed beds and possibly some field studies. The results of several simulations indicate that for short downstream distances, predictions of contaminant concentrations are sensitive to the source structure and orientation with respect to the direction of interstitial flow.

Introduction

As a substantial number of aquifers contaminated by nonaqueous phase liquids (NAPLs) have been identified and characterized, groundwater cleanup has reached significant proportions. Most of the NAPLs are organic solvents and petroleum hydrocarbons originating from leaking underground storage tanks, ruptured pipelines, surface spills, hazardous waste landfills, and disposal sites. As a NAPL is released into the subsurface environment, it infiltrates through the vadose zone, leaving behind blobs or ganglia which are no longer connected to the main body of the organic liquid. Upon reaching the water table, NAPLs lighter than water remain above the water table in the form of a floating pool; NAPLs heavier than water continue to migrate downward until they encounter an impermeable layer where a flat pool starts to form (see Figure 1). As groundwater flows past trapped ganglia or NAPL pools, a plume of dissolved hydrocarbons is created.

In recent years, numerous theoretical and experimental studies have focused on NAPL behavior in saturated porous media [*Fried et al.*, 1979; *Schwille*, 1988; *Powers et al.*, 1991, 1992; *Anderson et al.*, 1992a, b; *Borden and Piwoni*, 1992; *Conrad et al.*, 1992; *Johnson and Pankow*, 1992; *Thomson et al.*, 1992; *Geller and Hunt*, 1993; *Mayer and Miller*, 1993], unsaturated porous media [*van der Waarden et al.*, 1977; *Corapcioglu and Baehr*, 1987; *Baehr*, 1987; *Zalidis et al.*, 1991; *El-Kadi*, 1992; *Ostendorf et al.*, 1993; *Pantazidou and Sitar*, 1993], as well as in saturated/unsaturated multiphase systems [*Abriola and Pinder*, 1985; *Pinder and Abriola*, 1986]. However, the literature on groundwater contamination by pool dissolution of dense organic solvents is quite limited. *Hunt et al.* [1988] presented an analytical solution to the two-dimensional steady state advection-dispersion equation suitable for NAPL pool dissolution in saturated semi-infinite homogeneous porous media, making the assumption that the pool is of rectangular geometry and the dissolved solute is conservative. *Chrysikopoulos et al.* [1994], making the assumption that the dissolved solute decays and undergoes sorption governed by a linear equilibrium isotherm under local chemical equilibrium conditions, extended this model to account for transient contaminant transport from a single-component NAPL pool. *Anderson et al.* [1992b] presented a time dependent infinite series solution to a conservative single-contaminant pool dissolution in a three-dimensional homogeneous porous medium under steady unidirectional flow conditions. The models presented by *Hunt et al.* [1988] and *Chrysikopoulos et al.* [1994] assume that the source concentrations are equal to the solubility of the solvent. On the other hand, *Anderson et al.* [1992b] incorporated in their model an expression for a constant mass transfer flux (or in their terminology the surface area–averaged mass transfer rate [*Johnson and Pankow*, 1992]).

A NAPL spill is a very complicated phenomenon, but the objective here is to study a small part of this phenomenon, rather than to develop a comprehensive model for a NAPL spill. Specifically, this work focuses on the development of analytical solutions for the transient three-dimensional contaminant transport from a single-component NAPL pool in saturated homogeneous porous media under steady unidirectional flow conditions. Multicomponent NAPL pools raise a lot of other issues regarding solubility and equilibrium and are not examined here. The present work improves upon previously published mathematical models of NAPL pool dissolution, because the dissolution process is considered mass transfer limited and a variety of pool geometries (rectangular, elliptic, and circular) are examined. For mathematical simplicity it is hypothesized that the dissolved solute decays and undergoes sorption processes which are based on linear equilibrium isotherms and that the local chemical equilibrium assumption is valid. The use of a linear sorption isotherm is reasonable for

Paper number 94WR02780.
0043-1397/95/94WR-02780$02.00

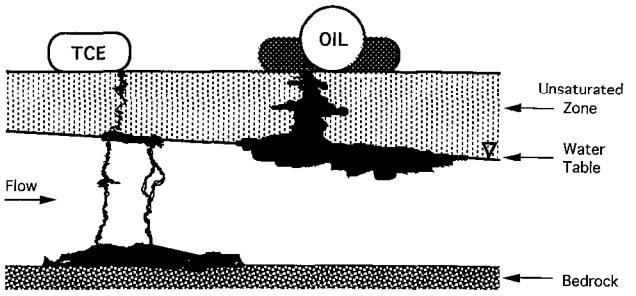

Figure 1. Schematic illustration of the migration in the subsurface of organic liquids that are slightly soluble in water, showing liquids that are heavier than water, such as trichloroethylene (TCE), and lighter than water petroleum products (oil).

low solute concentration which is frequently the case for many dissolving NAPLs [*Schwille*, 1988]. Furthermore, it is assumed that the aqueous phase concentration of the dissolved solute adjacent to the source is equal to its solubility limit. This equilibrium partitioning is based on the assumption that the characteristic timescale of the mass transfer process is much smaller than the characteristic timescale of the advective-dispersive transport. Such conditions have been observed by *van der Waarden et al.* [1971], *Fried et al.* [1979], *Schwille* [1984], and *Borden and Piwoni* [1992]. However, it should be noted that for some situations involving pools of irregular NAPL distribution or ganglia of certain blob sizes, equilibrium partitioning and solubility conditions may not be maintained [*Mackay et al.*, 1985; *Powers et al.*, 1991; *Geller and Hunt*, 1993]. From a mathematical modeling viewpoint this problem has similarities to the extensively investigated case of solute transport in multidimensional porous media [e.g., *Leij and Dane*, 1990]. Although the analytical models developed in this paper are for denser than water NAPL pools, these models can also be used for lighter than water NAPL pools by simply reversing the positive direction of the spatial coordinate z. Assuming that the NAPL-water interface is flat, complexities associated with lighter than water NAPL distribution at the capillary fringe are eliminated.

Development of Models

Rectangular Pool

The transient contaminant transport from a dissolving NAPL rectangular pool denser than water in a three-dimensional homogeneous porous medium under steady state uniform flow conditions as shown in Figure 2, assuming that the organic solvent is sorbing under local equilibrium conditions, is governed by

$$R\frac{\partial C(t,x,y,z)}{\partial t} = D_x\frac{\partial^2 C(t,x,y,z)}{\partial x^2} + D_y\frac{\partial^2 C(t,x,y,z)}{\partial y^2} + D_z\frac{\partial^2 C(t,x,y,z)}{\partial z^2} - U_x\frac{\partial C(t,x,y,z)}{\partial x} - \lambda RC(t,x,y,z), \quad (1)$$

where $C(t, x, y, z)$ is the liquid phase solute concentration; U_x is the average interstitial fluid velocity; x, y, z are the spatial coordinates in the longitudinal, lateral, and vertical directions, respectively; t is time; R is the dimensionless retardation factor for linear, reversible, instantaneous sorption; D_x, D_y, D_z are the longitudinal, lateral, and vertical hydrodynamic dispersion coefficients, respectively; and λ is a first-order decay constant. Assuming that the thickness of the pool is insignificant relative to the thickness of the aquifer and NAPL dissolution is described by the following mass transfer relationship, applicable at the NAPL-water interface,

$$-\mathcal{D}_e\frac{\partial C(t,x,y,0)}{\partial z} = k(t,x,y)[C_s - C(t,x,y,\infty)], \quad (2)$$

where $\mathcal{D}_e = \mathcal{D}/\tau^*$ is the effective molecular diffusion coefficient, $\mathcal{D}$ is the molecular diffusion coefficient, τ^* is the tortuosity coefficient ($\tau^* \geq 1$), $k(t, x, y)$ is the local mass transfer coefficient dependent on time and location on the NAPL-water interface (readers familiar with the study of heat transfer will realize that the local mass transfer coefficient is analogous to the time/space dependent local heat transfer coefficient), C_s is the aqueous concentration at the interface and for a pure organic liquid equals the liquid's aqueous saturation (solubility) concentration [*Fried et al.*, 1979; *Geller and Hunt*, 1993; *Seagren et al.*, 1994], and $C(t, x, y, \infty) \simeq 0$ corresponds to the contaminant concentration outside the boundary layer, the appropriate initial and boundary conditions for this system are

$$C(0,x,y,z) = 0, \quad (3)$$

$$C(t,\pm\infty,y,z) = 0, \quad (4)$$

$$C(t,x,\pm\infty,z) = 0, \quad (5)$$

$$\mathcal{D}_e\frac{\partial C(t,x,y,0)}{\partial z} = -k(t,x,y)C_s \quad (6a)$$

$$\ell_{x_0} < x < \ell_{x_0} + \ell_x, \qquad \ell_{y_0} < y < \ell_{y_0} + \ell_y$$

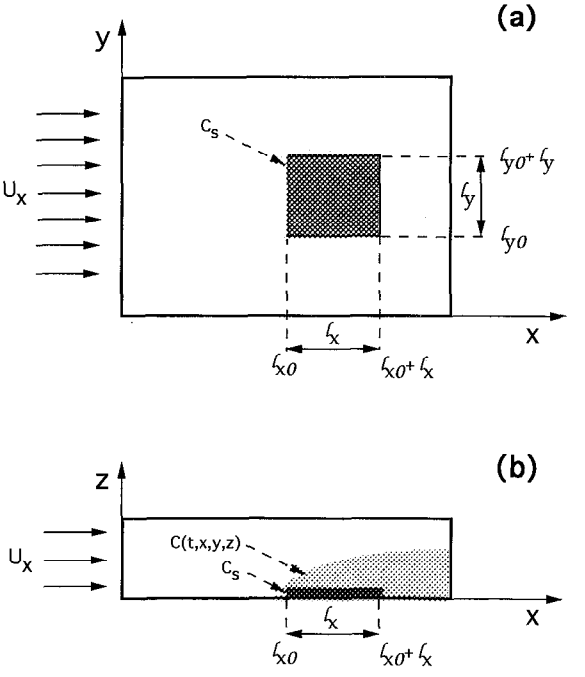

Figure 2. (a) Plan view of the conceptual model showing the unidirectional groundwater velocity U_x, the location of a denser than water NAPL pool with aqueous saturation concentration C_s and dimensions $\ell_x \times \ell_y$. (b) Profile view of the NAPL pool and the dissolved concentration $C(t, x, y, z)$.

$$\mathcal{D}_e \frac{\partial C(t, x, y, 0)}{\partial z} = 0 \qquad \text{otherwise,} \tag{6b}$$

$$C(t, x, y, \infty) = 0, \tag{7}$$

where ℓ_{x_0}, ℓ_{y_0} indicate the x, y Cartesian coordinates of the pool origin, respectively, and ℓ_x, ℓ_y are the pool dimensions in x, y directions, respectively. The concentration boundary layer implies that the dissolved concentration changes from the solubility concentration at the NAPL-water interface to the free-stream concentration in the interstitial fluid [*Bennett and Myers*, 1982, p. 551]. It should be noted that the decay term λRC in the governing equation (1) indicates that the total concentration (aqueous plus sorbed solute mass) disappears due to possible decay or biological/chemical degradation. A first-order decay term has also been used to determine many abiotic reactions and biological reactions at low concentrations [e.g., *van Genuchten*, 1981]. The aqueous saturation concentration (C_s) is kept constant at $z = 0$ because of the presence of NAPL phase in equilibrium with water at the interface. For a single-component NAPL, where no mass transfer limitations from within the NAPL occur, this is a reasonable boundary condition. If there is a decay, it is expected that the concentration profile with vertical distance from the NAPL would be different from that without decay, but both profiles would have $C = C_s$ at $z = 0$.

Taking Laplace transforms with respect to the variable t of (1), (6), and (7), applying initial condition (3), and taking double Fourier transforms of the resulting equations with respect to variables x, y yields

$$\frac{d^2\bar{C}^{\circ\bullet}(s, \gamma, \omega, z)}{dz^2} - \left(\frac{\gamma^2 D_x + \omega^2 D_y + i\gamma U_x + Rs + R\lambda}{D_z}\right) \cdot \bar{C}^{\circ\bullet}(s, \gamma, \omega, z) = 0, \tag{8}$$

$$\mathcal{D}_e \frac{d\bar{C}^{\circ\bullet}(s, \gamma, \omega, 0)}{dz} = -\frac{C_s}{2\pi}\int_{-\infty}^{\infty}\int_{-\infty}^{\infty} \bar{k}^{\circ\bullet}(s, \gamma - \alpha, \omega - \beta) \cdot \Phi^{\circ\bullet}(\alpha, \beta)\, d\beta\, d\alpha, \tag{9}$$

$$\bar{C}^{\circ\bullet}(s, \gamma, \omega, \infty) = 0, \tag{10}$$

where

$$\Phi^{\circ\bullet}(\gamma, \omega) = \left[\frac{e^{-i\gamma\ell_{x_0}} - e^{-i\gamma(\ell_{x_0}+\ell_x)}}{i\gamma(2\pi)^{1/2}}\right]\left[\frac{e^{-i\omega\ell_{y_0}} - e^{-i\omega(\ell_{y_0}+\ell_y)}}{i\omega(2\pi)^{1/2}}\right], \tag{11}$$

and the following definitions were employed for the Laplace and Fourier transformations [*Kreyszig*, 1993, p. 621]

$$\bar{C}(s, x, y, z) = \int_0^{\infty} C(t, x, y, z)e^{-st}\, dt, \tag{12}$$

$$\bar{C}^{\circ}(s, \gamma, y, z) = \frac{1}{(2\pi)^{1/2}}\int_{-\infty}^{\infty} \bar{C}(s, x, y, z)e^{-i\gamma x}\, dx, \tag{13}$$

$$\bar{C}^{\circ\bullet}(s, \gamma, \omega, z) = \frac{1}{(2\pi)^{1/2}}\int_{-\infty}^{\infty} \bar{C}^{\circ}(s, \gamma, y, z)e^{-i\omega y}\, dy, \tag{14}$$

$$\mathcal{F}\{f_1(x)f_2(x)\} = \frac{1}{(2\pi)^{1/2}} f_1^{\circ}(\gamma) * f_2^{\circ}(\gamma) = \frac{1}{(2\pi)^{1/2}}\int_{-\infty}^{\infty} f_1^{\circ}(\gamma - \alpha) f_2^{\circ}(\alpha)\, d\alpha, \tag{15}$$

the tilde signifies Laplace transform and s is the transformed time variable, the open and solid degree signs signify Fourier transforms with respect to space variables x and y with corresponding transformed spatial variables γ, ω, respectively, the asterisk indicates convolution, $\mathcal{F}$ is the Fourier operator, and $i = (-1)^{1/2}$.

The solution to the ordinary differential equation (8) is

$$\bar{C}^{\circ\bullet}(s, \gamma, \omega, z) = M(s, \gamma, \omega)e^{\zeta z} + N(s, \gamma, \omega)e^{-\zeta z} \tag{16}$$

where

$$\zeta = \left(\frac{R}{D_z}\right)^{1/2}\left(\frac{\gamma^2 D_x + \omega^2 D_y + i\gamma U_x}{R} + \lambda + s\right)^{1/2}, \tag{17}$$

and $M(s, \gamma, \omega)$, $N(s, \gamma, \omega)$ are Laplace/Fourier functions which must be evaluated from boundary conditions. Applying boundary condition (10) in (16) yields

$$M(s, \gamma, \omega) = 0. \tag{18}$$

In view of (9), (16), and (18) the unknown $N(s, \gamma, \omega)$ is evaluated to be

$$N(s, \gamma, \omega) = \frac{C_s}{2\pi\zeta\mathcal{D}_e}\int_{-\infty}^{\infty}\int_{-\infty}^{\infty} \bar{k}^{\circ\bullet}(s, \gamma - \alpha, \omega - \beta) \cdot \Phi^{\circ\bullet}(\alpha, \beta)\, d\beta\, d\alpha. \tag{19}$$

Substituting (18) and (19) into (16) leads to

$$\bar{C}^{\circ\bullet}(s, \gamma, \omega, z) = \frac{C_s e^{-\zeta z}}{2\pi\zeta\mathcal{D}_e}\int_{-\infty}^{\infty}\int_{-\infty}^{\infty} \bar{k}^{\circ\bullet}(s, \gamma - \alpha, \omega - \beta) \cdot \Phi^{\circ\bullet}(\alpha, \beta)\, d\beta\, d\alpha. \tag{20}$$

Following the procedure outlined by *Chrysikopoulos et al.* [1994] the inverse Laplace transformation with respect to s and the inverse Fourier transformation with respect to γ of the preceding equation can be obtained as

$$C^{\bullet}(t, x, \omega, z) = \frac{-C_s}{2^{1/2}\pi\mathcal{D}_e}\int_0^t\int_{\kappa_1}^{\kappa_2}\int_{-\infty}^{\infty}\left(\frac{D_z}{R\pi\tau}\right)^{1/2} \cdot k^{\bullet}(t - \tau, u, \omega - \beta)\left[\frac{e^{-i\beta\ell_{y_0}} - e^{-i\beta(\ell_{y_0}+\ell_y)}}{i\beta(2\pi)^{1/2}}\right] \cdot \exp\left[-\frac{\omega^2 D_y\tau}{R} - \lambda\tau - \frac{Rz^2}{4D_z\tau}\right] \exp[-\eta^2]\, d\beta\, d\eta\, d\tau, \tag{21}$$

where

$$\kappa_1 = [x - \ell_{x_0} - (U_x\tau/R)](R/4D_x\tau)^{1/2}, \tag{22}$$

$$\kappa_2 = [x - \ell_{x_0} - \ell_x - (U_x\tau/R)](R/4D_x\tau)^{1/2}, \tag{23}$$

$$\eta = [x - (U_x\tau/R) - u](R/4D_x\tau)^{1/2}. \tag{24}$$

To determine the inverse Fourier transformation of (21) with respect to ω, define the functions $f(y)$ and $g(y)$ as follows:

$$f(y) = \mathcal{F}^{-1}\left\{\exp\left[-\frac{\omega^2 D_y \tau}{R}\right]\right\} = \left(\frac{R}{2D_y\tau}\right)^{1/2} \exp\left[-\frac{Ry^2}{4D_y\tau}\right], \tag{25}$$

$$g(y) = \mathcal{F}^{-1}\left\{\frac{1}{(2\pi)^{1/2}}\int_{-\infty}^{\infty} k^*(t-\tau, u, \omega-\beta) \cdot \left[\frac{e^{-i\beta\ell_{y_0}} - e^{-i\beta(\ell_{y_0}+\ell_y)}}{i\beta(2\pi)^{1/2}}\right] d\beta\right\} = k(t-\tau, u, y) \tag{26a}$$

$$\ell_{y_0} < y < \ell_{y_0} + \ell_y,$$

$$g(y) = 0 \qquad \text{otherwise.} \tag{26b}$$

Direct application of the convolution theorem and substitution of $f(y)$ and $g(y)$ leads to

$$\mathcal{F}^{-1}\{f^*(\omega)g^*(\omega)\} = \frac{1}{(2\pi)^{1/2}}\int_{-\infty}^{\infty} f(y-v)g(v)\,dv = \frac{1}{(2\pi)^{1/2}}\int_{\ell_{y_0}}^{\ell_{y_0}+\ell_y}\left(\frac{R}{2D_y\tau}\right)^{1/2} k(t-\tau, u, v) \cdot \exp\left[-\frac{R(y-v)^2}{4D_y\tau}\right] dv, \tag{27}$$

where v is a dummy integration variable. Substituting the following expression

$$\mu = (y-v)(R/4D_y\tau)^{1/2}, \tag{28}$$

into (27) yields

$$\mathcal{F}^{-1}\{f^*(\omega)g^*(\omega)\} = \frac{-1}{\pi^{1/2}}\int_{\xi_1}^{\xi_2} k(t-\tau, u, v)\exp[-\mu^2]\,d\mu, \tag{29}$$

where

$$\xi_1 = (y-\ell_{y_0})(R/4D_y\tau)^{1/2}, \tag{30}$$

$$\xi_2 = (y-\ell_{y_0}-\ell_y)(R/4D_y\tau)^{1/2}. \tag{31}$$

In view of (21), (25), (26), and (29), the desired expression for $C(t, x, y, z)$ is

$$C(t,x,y,z) = \frac{C_s}{\pi\mathcal{D}_e}\int_0^t\int_{\kappa_1}^{\kappa_2}\int_{\xi_1}^{\xi_2}\left(\frac{D_z}{R\pi\tau}\right)^{1/2} k(t-\tau, u, v) \cdot \exp\left[-\lambda\tau - \frac{Rz^2}{4D_z\tau}\right]\exp[-\eta^2]\exp[-\mu^2]\,d\mu\,d\eta\,d\tau, \tag{32}$$

where u and v are obtained from (24) and (28), respectively, as

$$u = x - (U_x\tau/R) - \eta(4D_x\tau/R)^{1/2}, \tag{33}$$

$$v = y - \mu(4D_y\tau/R)^{1/2}. \tag{34}$$

For the special case where the local mass transfer coefficient can be replaced by an average (or overall) mass transfer coefficient $k(t, x, y) = k^*$, the general solution (32) is simplified to the following expression:

$$C(t,x,y,z) = \frac{C_s k^*}{4\mathcal{D}_e}\int_0^t\left(\frac{D_z}{R\pi\tau}\right)^{1/2}\exp\left[-\lambda\tau - \frac{Rz^2}{4D_z\tau}\right] \cdot [\operatorname{erf}(\kappa_1) - \operatorname{erf}(\kappa_2)][\operatorname{erf}(\xi_1) - \operatorname{erf}(\xi_2)]\,d\tau, \tag{35}$$

where the definition and fundamental properties of the error function have been employed for the evaluation of the integrals [*Gautschi*, 1972], in conjunction with (22), (23), (30), and (31). For a rectangular pool of infinite lateral extent ($\ell_{y_0} = -\infty$ and $y = \infty$), (35) reduces to the two-dimensional model presented by *Chrysikopoulos et al.* [1994].

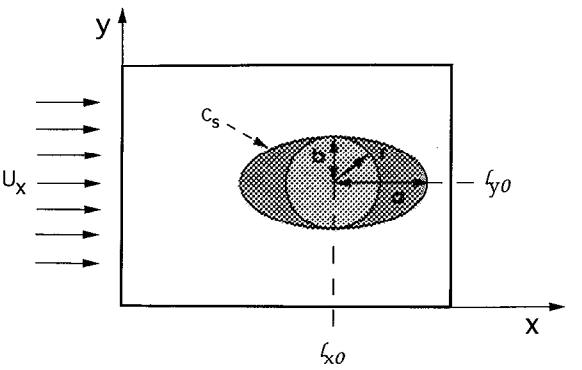

Figure 3. Plan view of a denser than water elliptic pool with origin at $x = \ell_{x_0}$, $y = \ell_{y_0}$, having major semiaxis a and minor semiaxis b. For the special case where $a = b = r$ the elliptic pool becomes a circular pool with radius r.

Elliptic Pool

For a NAPL pool of elliptic shape, as shown in Figure 3, the appropriate source boundary condition is

$$\mathcal{D}_e\frac{\partial C(t,x,y,0)}{\partial z} = -k(t,x,y)C_s \qquad (x-\ell_{x_0})^2/a^2 + (y-\ell_{y_0})^2/b^2 \le 1, \tag{36a}$$

$$\mathcal{D}_e\frac{\partial C(t,x,y,0)}{\partial z} = 0 \qquad (x-\ell_{x_0})^2/a^2 + (y-\ell_{y_0})^2/b^2 > 1, \tag{36b}$$

where a, b are the major and minor semiaxes of the elliptic pool, respectively. Taking Laplace transforms with respect to the variable t and Fourier transforms with respect to space variables x and y of the preceding equation yields

$$\mathcal{D}_e\frac{d\bar{C}^{**}(s,\gamma,\omega,0)}{dz} = -\frac{C_s}{2\pi}\int_{-\infty}^{\infty}\int_{-\infty}^{\infty}\bar{k}^{**}(s,\gamma-\alpha,\omega-\beta) \cdot \Omega^{**}(\alpha,\beta)\,d\beta\,d\alpha, \tag{37}$$

where $\Omega^{**}(\gamma, \omega)$ is the double Fourier transform of

$$\Omega(x,y) = 1 \qquad (x-\ell_{x_0})^2/a^2 + (y-\ell_{y_0})^2/b^2 \le 1, \tag{38a}$$

$$\Omega(x,y) = 0 \qquad (x-\ell_{x_0})^2/a^2 + (y-\ell_{y_0})^2/b^2 > 1. \tag{38b}$$

Although an explicit expression for $\Omega^{**}(\gamma, \omega)$ can be obtained, for mathematical convenience it is considered as an unknown function.

The solution to the ordinary differential equation (8) subject to (37) followed by inverse Laplace transform with respect to s is

$$C^{\circ\bullet}(t,\gamma,\omega,z)=\frac{C_s}{2\pi\mathcal{D}_e}\int_0^t\int_{-\infty}^{\infty}\int_{-\infty}^{\infty}\left(\frac{D_z}{R\pi\tau}\right)^{1/2}\cdot k^{\circ\bullet}(t-\tau,\gamma-\alpha,\omega-\beta)\Omega^{\circ\bullet}(\alpha,\beta)\cdot\exp\left[-\frac{(\gamma^2D_x+\omega^2D_y+i\gamma U_x)\tau}{R}-\lambda\tau-\frac{Rz^2}{4D_z\tau}\right]\cdot d\beta\,d\alpha\,d\tau. \tag{39}$$

Using the convolution theorem, the inverse Fourier transformation with respect to γ of the preceding equation is determined as

$$C^{\bullet}(t,x,\omega,z)=\frac{C_s}{2\pi\mathcal{D}_e}\int_0^t\int_{-\infty}^{\infty}\int_{-\infty}^{\infty}\cdot\left(\frac{D_z}{2\pi D_x\tau^2}\right)^{1/2}k^{\bullet}(t-\tau,u,\omega-\beta)\Omega^{\bullet}(u,\beta)\cdot\exp\left[-\frac{\omega^2D_y\tau}{R}-\lambda\tau-\frac{Rz^2}{4D_z\tau}\right]\cdot\exp\left[-\frac{R}{4D_x\tau}\left(x-\frac{U_x\tau}{R}-u\right)^2\right]d\beta\,du\,d\tau, \tag{40}$$

where the following shifting property has been employed [*Kreyszig*, 1993, p. 618]

$$\mathcal{F}^{-1}\{f^{\circ}(\gamma)e^{-i\gamma d}\}=f(x-d), \tag{41a}$$

with

$$d=U_x\tau/R. \tag{41b}$$

The inverse Fourier transformation of (40) with respect to ω is obtained also by application of the convolution theorem to yield

$$C(t,x,y,z)=\frac{C_s}{2\pi\mathcal{D}_e}\int_0^t\int_{-\infty}^{\infty}\int_{-\infty}^{\infty}\left(\frac{D_zR}{4\pi D_xD_y\tau^3}\right)^{1/2}\cdot k(t-\tau,u,v)\Omega(u,v)\exp\left[-\lambda\tau-\frac{Rz^2}{4D_z\tau}\right]\cdot\exp\left[-\frac{R}{4D_x\tau}\left(x-\frac{U_x\tau}{R}-u\right)^2\right]\cdot\exp\left[-\frac{R(y-v)^2}{4D_y\tau}\right]dv\,du\,d\tau, \tag{42}$$

where v is a dummy integration variable.

In view of (24), (28), and (38), equation (42) can be written as

$$C(t,x,y,z)=\frac{C_s}{\pi\mathcal{D}_e}\int_0^t\int_{n_1}^{n_2}\int_{m_1}^{m_2}\left(\frac{D_z}{\pi R\tau}\right)^{1/2}k(t-\tau,u,v)\cdot\exp\left[-\lambda\tau-\frac{Rz^2}{4D_z\tau}\right]\exp[-\eta^2]\exp[-\mu^2]\,d\mu\,d\eta\,d\tau, \tag{43}$$

where

$$m_1=(y-\ell_{y_0}+b)(R/4D_y\tau)^{1/2}, \tag{44}$$

$$m_2=(y-\ell_{y_0}-b)(R/4D_y\tau)^{1/2}, \tag{45}$$

$$n_1=\left[x-\frac{U_x\tau}{R}-\ell_{x_0}+\left\{\left[1-\frac{(v-\ell_{y_0})^2}{b^2}\right]a^2\right\}^{1/2}\right]\cdot\left(\frac{R}{4D_x\tau}\right)^{1/2}, \tag{46}$$

$$n_2=\left[x-\frac{U_x\tau}{R}-\ell_{x_0}-\left\{\left[1-\frac{(v-\ell_{y_0})^2}{b^2}\right]a^2\right\}^{1/2}\right]\cdot\left(\frac{R}{4D_x\tau}\right)^{1/2}, \tag{47}$$

and u and v are defined in (33) and (34), respectively.

For the special case of an average mass transfer coefficient $k(t,x,y)=k^*$, we can simplify the general solution (43) to the following expression:

$$C(t,x,y,z)=\frac{C_sk^*}{2\pi\mathcal{D}_e}\int_0^t\int_{m_1}^{m_2}\left(\frac{D_z}{R\tau}\right)^{1/2}\exp\left[-\lambda\tau-\frac{Rz^2}{4D_z\tau}\right]\cdot\exp[-\mu^2](\operatorname{erf}[n_2]-\operatorname{erf}[n_1])\,d\mu\,d\tau, \tag{48}$$

where the integration with respect to η has been eliminated by employing the definition of the error function.

Circular Pool

A circular pool with radius r, as shown in Figure 3, is equivalent to an elliptic pool when $a=b=r$. Since the circular pool geometry is a special case of an elliptic pool, the appropriate source boundary condition for a circular pool is obtained by setting $a=b=r$ in (36). Furthermore, the general solution to the circular pool problem as well as the corresponding solution to the case where $k(t,x,y)=k^*$, can be obtained directly from (43) and (48), respectively, by substituting $a=b=r$.

Discussion

The problem of contaminant transport from single-component NAPL pool dissolution in homogeneous porous media is examined for the general case of a local mass transfer coefficient dependent on time and location on the NAPL-water interface. The closed form analytical solutions derived for rectangular and elliptic/circular pool geometries are given by (32) and (43), respectively. The time and space dependence of the local mass transfer coefficient can only be determined experimentally; however, such information is not currently available in the published literature. For computational purposes, $k(t,x,y)$ is replaced by an average (or overall) mass transfer coefficient k^*, which can be considered as a curve-fitting parameter, and the analytical solutions for rectangular and elliptic/circular pool geometries are further simplified to (35) and (48), respectively. All simulations presented in this section are based on the analytical solutions derived for the case of an average mass transfer coefficient. The model parameters used for the simulations are listed in Table 1. These parameters, with the exception of U_x and D_z, represent the conditions of a laboratory experiment of 1,1,2-trichloroethane (TCA) transport resulting

Table 1. Model Parameters for Simulations

Parameter	Value
$\mathcal{D}_e$	2.04×10^{-6} m^2/h
D_x	1.14×10^{-5} m^2/h
$D_y = D_z$	2.04×10^{-6} m^2/h
k^*	9.78×10^{-5} m/h
R	1.1
U_x	0.035 m/h
λ	0.0 h^{-1}

from dissolution of a two-dimensional pool [*Chrysikopoulos et al.*, 1994]. All integrals are evaluated numerically by the extended Simpson's rule [*Press et al.*, 1992].

For the case of a rectangular NAPL pool, the analytical solution (35) is employed to simulate contaminant concentration distributions in a hypothetical three-dimensional homogeneous porous formation for two different points in time. For presentation purposes the concentrations presented in the figures are normalized by the solvent's aqueous saturation concentration. Figure 4 illustrates concentration contours in the xy plane at a vertical height of 0.02 m above the rectangular NAPL pool for 100 and 500 hours from the initiation of the dissolution process. Similarly, Figure 5 illustrates concentration contours in the xz plane along the centerline of the pool in the downstream direction ($y = 3.5$) for the same model parameters and the corresponding times given in Figure 4. The concentration contour plots illustrate the evolution of the contaminant plume and show, as intuitively expected, that concentration levels decline with increasing longitudinal and vertical distance from the rectangular pool.

The effects of the model parameters, interstitial velocity, dispersion coefficients, retardation factor, and first-order decay

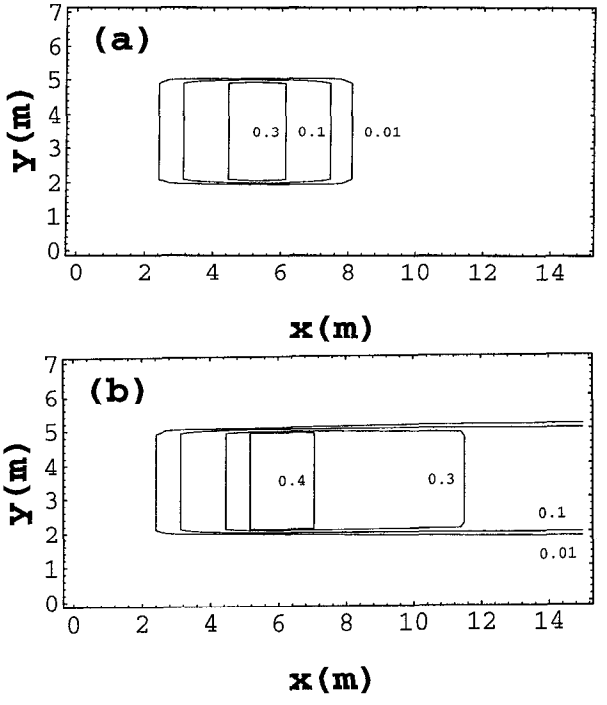

Figure 4. Normalized concentration contours in the xy plane at (a) $t = 100$ hours and (b) $t = 500$ hours. (Here $\ell_x = \ell_y = 3$ m, $\ell_{x_0} = \ell_{y_0} = 2$ m, $z = 0.02$ m.)

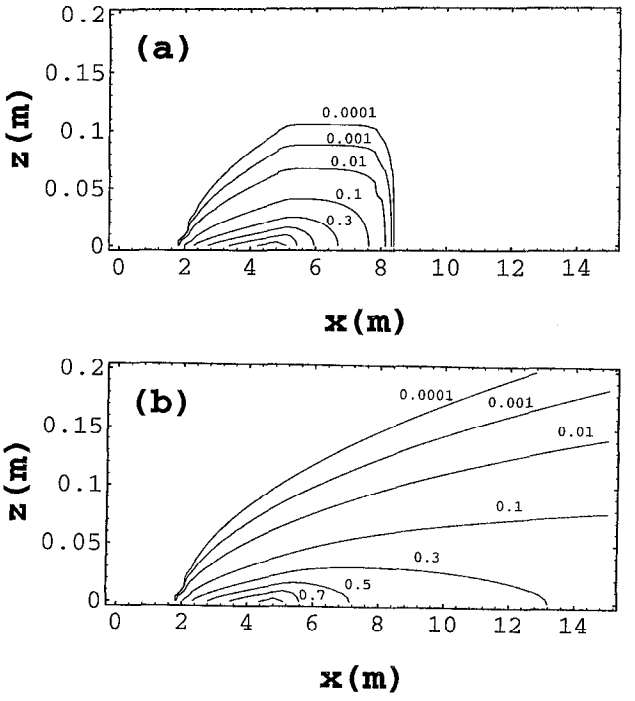

Figure 5. Normalized concentration contours in the xz plane at (a) $t = 100$ hours and (b) $t = 500$ hours. (Here $\ell_x = \ell_y = 3$ m, $\ell_{x_0} = \ell_{y_0} = 2$ m, $y = 3.5$ m.)

coefficient on the transport of the dissolved contaminant are not graphically presented here, because they have been investigated extensively in earlier contaminant transport studies. It should be noted, however, that at early time, dissolved contaminant concentrations decrease with increasing retardation factor. At large time the magnitude of the retardation factor no longer affects the concentration distributions for the case where $\lambda = 0$, but for $\lambda \neq 0$ the dissolved concentrations are dependent on R. Thus for a decaying solvent the dissolved concentration distributions are dependent on the retardation factor at all times.

Figure 6 shows contaminant concentration profiles, simulated with (35), along the rectangular pool centerline in the downstream direction at $z = 0.04$ m from three NAPL pool sources of equal surface area with dimensions $\ell_x \times \ell_y$ of 1×9 m^2, 3×3 m^2, and 9×1 m^2, respectively. It is evident that the source structure and orientation control the magnitude of the dissolved contaminant concentration. The longer the pool in the direction of flow, the higher the solute peak concentration in the interstitial fluid. The wider the pool perpendicular to the direction of flow, the larger the immediate downstream area covered by the dissolved contaminant.

The curves in Figure 7 are constructed with (48) and illustrate the effect of Sherwood number and eccentricity of an elliptic NAPL pool on dissolved contaminant concentration. The Sherwood number is defined as

$$Sh_0 = k^* \ell / \mathcal{D}_e, \tag{49}$$

where ℓ is the maximum pool length in the direction of flow (for an elliptic pool $\ell = 2a$ is the major axis), whereas the eccentricity of an elliptic pool is defined as

$$\varepsilon = [1 - (b/a)^2]^{1/2}. \tag{50}$$

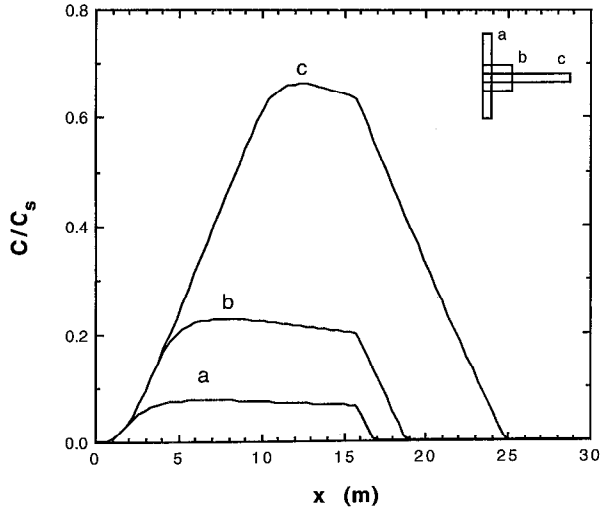

Figure 6. Distribution of normalized concentration versus downstream distance for pools of equal surface area and dimensions $\ell_x \times \ell_y$ of 1×9 m^2 (curve a), 3×3 m^2 (curve b), and 9×1 m^2 (curve c). (Here $\ell_{x_0} = 0$ m, $\ell_{y_0} = 0$, 3, 4 m for curves a, b, and c, respectively, $y = 4.5$ m, $z = 0.04$ m.)

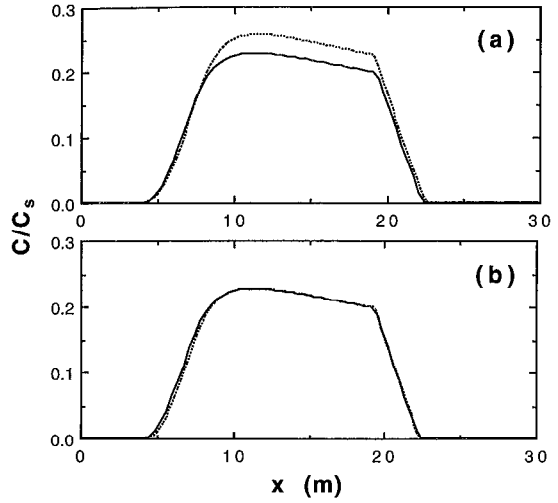

Figure 8. Distribution of normalized concentration versus downstream distance for pools of rectangular (solid lines) and circular (dotted lines) geometry for the cases of (a) equal surface area: $\ell_x = \ell_y = 3$ m, $r = (\ell_x \ell_y/\pi)^{1/2}$ and (b) equal longitudinal length: $\ell_x = \ell_y = 2r = 3$ m. (Here $\ell_{x_0} = \ell_{y_0} = 3.5$, 5 m for the rectangular and circular pool, respectively, $y = 5$ m, $z = 0.04$ m.)

When $\varepsilon = 0$, then $a = b$ and the elliptic pool becomes circular. The closer ε is to 1, the more elongated the elliptic pool. Figure 7 shows a linear relationship between Sh_0 and $C(t, x, y, z)$, and indicates that the dissolved contaminant concentration at $(x, y, z) = (10, 5, 0.04$ m) within the three-dimensional homogeneous porous formation is increasing with increasing Sh_0 or ε. For a fixed $\mathcal{D}_e$, an increase in Sh_0 suggests an increase in k^* or an increase in ℓ. An increase in ε suggests an increase in a and consequently an increase in ℓ. Therefore an increase in ε also implies an increase in Sh_0. The result of Figure 7 is in agreement with that of Figure 6.

In real situations the geometry of a NAPL pool is seldom known with any accuracy. To examine the effect of pool geometry on dissolved concentration levels, simulations for rectangular pools using (35) and circular pools using (48) (with $a = b = r$) are compared in Figure 8. For the case of NAPL pools of equal surface area, the dissolved contaminant concentration along the centerline of the source in the downstream direction is higher for the circular pool geometry. This is attributed to the fact that the diameter of the circular pool is greater than the side of the rectangular pool of equal surface area. Therefore the source with the longer length along the flow direction leads to higher peak concentrations. If the diameter of the circular pool is equal to the side of the rectangular pool, the two concentration profiles predicted by the models are identical (see Figure 8b). Obviously, these results are valid only at the centerline of the two NAPL pools. It should be noted that Figures 8a and 8b are constructed assuming that the centers of the two pools coincide.

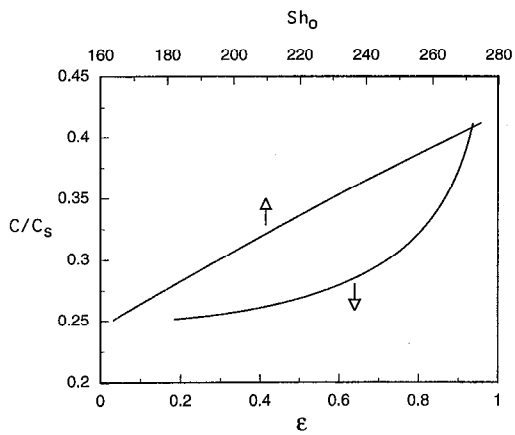

Figure 7. Sherwood number and eccentricity of an elliptic pool versus dissolved normalized concentration at a location with coordinates $(x, y, z) = (10, 5, 0.04$ m). (Here $\ell_{x_0} = \ell_{y_0} = 5$ m.)

Summary and Concluding Remarks

The primary contribution of this work is the development of analytical solutions for contaminant transport from NAPL pool dissolution in three-dimensional, homogeneous, saturated porous media. The solutions were obtained by employing a Laplace transform with respect to t and double Fourier transforms with respect to x and y, for rectangular and elliptic, as well as circular NAPL pools. The aqueous phase concentration of the dissolved solute adjacent to the source is considered to be equal to the solubility limit, and the dissolution process is mass transfer limited. The analytical solutions are useful for design and interpretation of experiments in laboratory-packed beds and possibly some homogeneous aquifers and for the verification of complex numerical models. It was demonstrated through synthetic examples that the more elongated the pool along the direction of the interstitial flow, the higher the dissolved peak concentration. Furthermore, it was shown that the dissolved contaminant concentration is proportional to the Sherwood number.

Notation

a, b major and minor semiaxes of elliptic pool, respectively, L.
C liquid phase solute concentration (solute mass/liquid volume), M/L^3.
C_s aqueous saturation concentration (solubility), M/L^3.
d defined in (41b).
$\mathcal{D}$ molecular diffusion coefficient, L^2/t.
$\mathcal{D}_e$ effective molecular diffusion coefficient, equal to $\mathcal{D}/\tau^*$, L^2/t.
D_x longitudinal hydrodynamic dispersion coefficient, L^2/t.
D_y lateral hydrodynamic dispersion coefficient, L^2/t.
D_z hydrodynamic dispersion coefficient in the vertical direction, L^2/t.
$\text{erf}[x]$ error function, equal to $(2/\pi^{1/2}) \int_0^x e^{-z^2}\, dz$.
f defined in (25).
$\mathcal{F}$ Fourier operator.
$\mathcal{F}^{-1}$ Fourier inverse operator.
g defined in (26).
k local mass transfer coefficient, L/t.
k^* average mass transfer coefficient, L/t.
ℓ maximum pool length in the direction of flow, L.
ℓ_x, ℓ_y pool dimensions in x and y directions, respectively, L.
ℓ_{x_0}, ℓ_{y_0} x and y Cartesian coordinates, respectively, of the origin of a rectangular pool or the center of an elliptic/circular pool, L.
m_1, m_2 defined in (44) and (45), respectively.
M Laplace/Fourier function defined in (18).
n_1, n_2 defined in (46) and (47), respectively.
N Laplace/Fourier function defined in (19).
r radius of circular pool, L.
R retardation factor.
s Laplace transform variable.
Sh_0 overall Sherwood number, equal to $k^*\ell/\mathcal{D}_e$.
t time, t.
u defined in (33).
U_x average interstitial velocity, L/t.
v defined in (34).
x, y, z spatial coordinates, L.
α, β dummy integration variables.
γ Fourier transform variable.
ε eccentricity of an elliptic pool, equal to $[1 - (b/a)^2]^{1/2}$.
ζ defined in (17).
η defined in (24).
κ_1, κ_2 defined in (22) and (23), respectively.
λ decay coefficient, t^{-1}.
μ defined in (28).
ξ_1, ξ_2 defined in (30) and (31), respectively.
τ dummy integration variable.
τ^* tortuosity factor (≥ 1).
$\Phi^{\circ\bullet}$ defined in (11).
ω Fourier transform variable.
Ω defined in (38).

Acknowledgments. This research was sponsored by the National Science Foundation, under grant BCS-9022205. The author thanks Marios Fyrillas, Maria Koundoura, Youn Sim, and Evangelos Voudrias for their contributions to this study.

References

Abriola, L. M., and G. F. Pinder, A multiphase approach to the modeling of porous media contamination by organic compounds, 1, Equation development, *Water Resour. Res.*, *21*(1), 11–18, 1985.
Anderson, M. R., R. L. Johnson, and J. F. Pankow, Dissolution of dense chlorinated solvents into groundwater, 1, Dissolution from a well-defined residual source, *Ground Water*, *30*(2), 250–256, 1992a.
Anderson, M. R., R. L. Johnson, and J. F. Pankow, Dissolution of dense chlorinated solvents into groundwater, 3, Modeling contaminant plumes from fingers and pools of solvent, *Environ. Sci. Technol.*, *26*(5), 901–908, 1992b.
Baehr, A. L., Selective transport of hydrocarbons in the unsaturated zone due to aqueous and vapor phase partitioning, *Water Resour. Res.*, *23*(10), 1926–1938, 1987.
Bennett, C. O., and J. E. Myers, *Momentum, Heat, and Mass Transfer*, 3rd ed., 832 pp., McGraw-Hill, New York, 1982.
Borden, R. C., and M. D. Piwoni, Hydrocarbon dissolution and transport: A comparison of equilibrium and kinetic models, *J. Contam. Hydrol.*, *10*, 309–323, 1992.
Chrysikopoulos, C. V., E. A. Voudrias, and M. M. Fyrillas, Modeling of contaminant transport resulting from dissolution of nonaqueous phase liquid pools in saturated porous media, *Transp. Porous Media*, *16*(2), 125–145, 1994.
Conrad, S. H., J. L. Wilson, W. R. Mason, and W. J. Peplinski, Visualization of residual organic liquid trapped in aquifers, *Water Resour. Res.*, *28*(2), 467–478, 1992.
Corapcioglu, M. Y., and A. L. Baehr, A compositional multiphase model for groundwater contamination by petroleum products, 1, Theoretical considerations, *Water Resour. Res.*, *23*(1), 191–200, 1987.
El-Kadi, A. I., Applicability of sharp-interface models for NAPL transport, 1, Infiltration, *Ground Water*, *30*(6), 849–856, 1992.
Fried, J. J., P. Muntzer, and L. Zilliox, Ground-water pollution by transfer of oil hydrocarbons, *Ground Water*, *17*(6), 586–594, 1979.
Gautschi, W., Error function and Fresnel integrals, in *Handbook of Mathematical Functions*, edited by M. Abramowitz and I. A. Stegun, pp. 209–329, Wiley-Interscience, New York, 1972.
Geller, J. T., and J. R. Hunt, Mass transfer from nonaqueous phase organic liquids in water-saturated porous media, *Water Resour. Res.*, *29*(4), 833–845, 1993.
Hunt, J. R., N. Sitar, and K. S. Udell, Nonaqueous phase liquid transport and cleanup, 1, Analysis of mechanisms, *Water Resour. Res.*, *24*(8), 1247–1258, 1988.
Johnson, R. L., and J. F. Pankow, Dissolution of dense chlorinated solvents into groundwater, 2, Source functions for pools of solvent, *Environ. Sci. Technol.*, *26*(5), 896–901, 1992.
Kreyszig, E., *Advanced Engineering Mathematics*, 7th ed., 1271 pp., John Wiley, New York, 1993.
Leij, F. J., and J. H. Dane, Analytical solution of the one-dimensional advection equation and two- or three-dimensional dispersion equation, *Water Resour. Res.*, *26*(7), 1475–1482, 1990.
Mackay, D. M., P. V. Roberts, and J. A. Cherry, Transport of organic contaminants in groundwater: Distribution and fate of chemicals in sand and gravel aquifers, *Environ. Sci. Technol.*, *19*(5), 384–392, 1985.
Mayer, A. S., and C. T. Miller, An experimental investigation of pore-scale distributions of nonaqueous phase liquids at residual saturation, *Transp. Porous Media*, *10*, 57–80, 1993.
Ostendorf, D. W., R. J. Richards, and F. P. Beck, LNAPL retention in sandy soil, *Ground Water*, *31*(2), 285–292, 1993.
Pantazidou, M., and N. Sitar, Emplacement of nonaqueous liquids in the vadose zone, *Water Resour. Res.*, *29*(3), 705–722, 1993.
Pinder, G. F., and L. M. Abriola, On the simulation of nonaqueous phase organic compounds in the subsurface, *Water Resour. Res.*, *22*(9), 109S–119S, 1986.
Powers, S. E., C. O. Loureiro, L. M. Abriola, and W. J. Weber Jr., Theoretical study of the significance of nonequilibrium dissolution of nonaqueous phase liquids in subsurface systems, *Water Resour. Res.*, *27*(4), 463–477, 1991.
Powers, S. E., L. M. Abriola, and W. J. Weber Jr., An experimental investigation of nonaqueous phase liquid dissolution in saturated subsurface systems: Steady state mass transfer rates, *Water Resour. Res.*, *28*(10), 2691–2705, 1992.
Press, W. H., B. P. Flannery, S. A. Teukolsky, and W. T. Vetterling, *Numerical Recipes: The Art of Scientific Computing*, 2nd ed., 963 pp., Cambridge University Press, New York, 1992.
Schwille, F., Migration of organic fluids immiscible with water in the

unsaturated zone, in *Pollutants in Porous Media: The Unsaturated Zone Between Soil Surface and Groundwater*, edited by B. Yaron, G. Dagan, and J. Goldshmid, pp. 27–48, Springer-Verlag, New York, 1984.

Schwille, F., *Dense Chlorinated Solvents in Porous and Fractured Media*, translated from German by J. F. Pankow, 146 pp., Lewis, Chelsea, Mich., 1988.

Seagren, E. A., B. E. Rittmann, and A. J. Valocchi, Quantitative evaluation of the enhancement of NAPL-pool dissolution by flushing and biodegradation, *Environ. Sci. Technol.*, *28*, 833–839, 1994.

Thomson, N. R., D. N. Graham, and G. J. Farquhar, One-dimensional immiscible displacement experiments, *J. Contam. Hydrol.*, *10*, 197–223, 1992.

van der Waarden, M., A. L. A. M. Bridié, and W. M. Groenewoud, Transport of mineral oil components to groundwater, 1, Model experiments on the transfer of hydrocarbons from a residual oil zone to trickling water, *Water Res.*, *5*, 213–226, 1971.

van der Waarden, M., W. M. Groenewoud, and A. L. A. M. Bridié, Transport of mineral oil components to groundwater, 2, Influence of lime, clay and organic soil components on the rate of transport, *Water Res.*, *11*, 359–365, 1977.

van Genuchten, M. T., Analytical solutions for chemical transport with simultaneous adsorption, zero-order production and first-order decay, *J. Hydrol.*, *49*, 213–233, 1981.

Zalidis, G. C., M. D. Annable, R. B. Wallace, N. J. Hayden, and T. C. Voice, A laboratory method for studying the aqueous phase transport of dissolved constituents from residually held NAPL in unsaturated soil columns, *J. Contam. Hydrol.*, *8*, 143–156, 1991.

C. V. Chrysikopoulos, Department of Civil and Environmental Engineering, University of California, Irvine, CA 92717.

(Received January 10, 1994; revised October 20, 1994;
accepted October 24, 1994.)